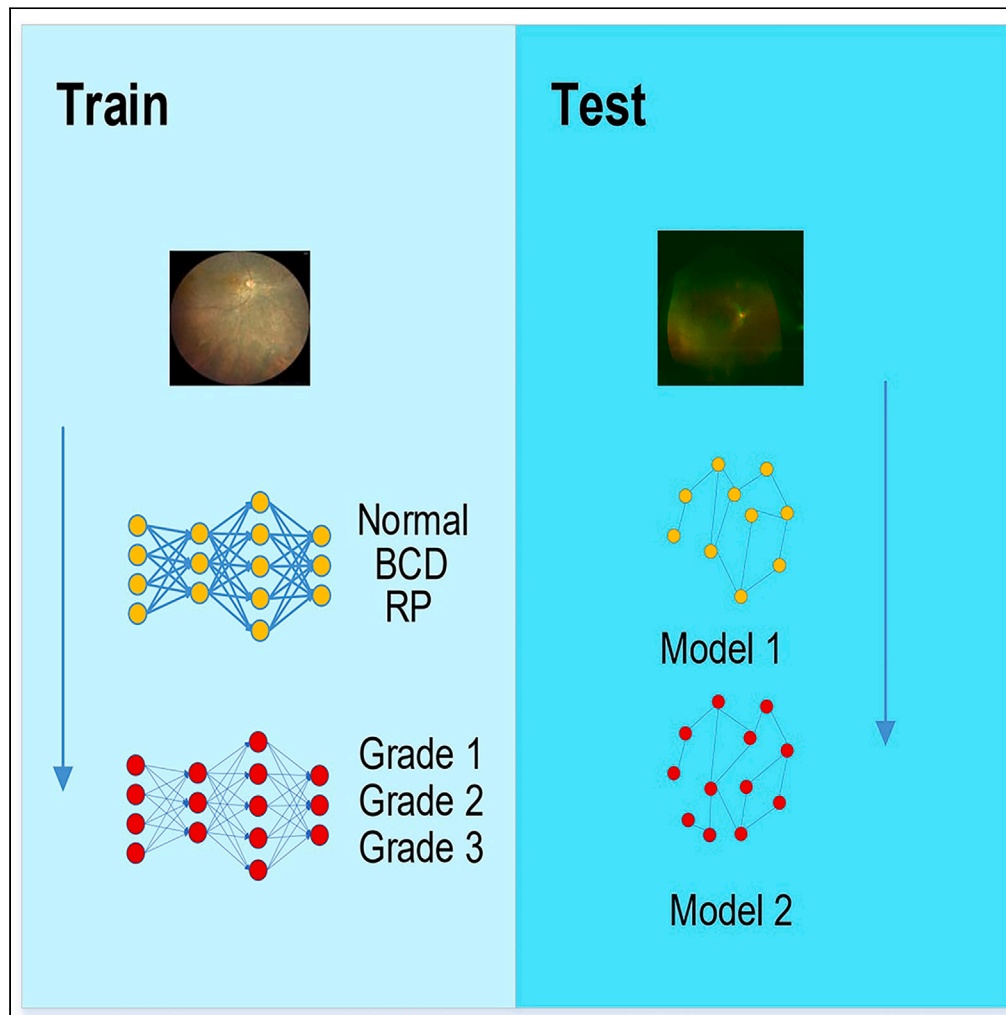# iScience

Article

Quickly diagnosing Bietti crystalline dystrophy with deep learning

Haihan Zhang, Kai Zhang, Jinyuan Wang, ..., Shiyi Yin, Jingyuan Zhu, Wenbin Wei

weiwenbintr@163.com

Highlights

Deep learning can automatically diagnose Bietti crystalline dystrophy (BCD)

Accurate classification of clinical stages allows for timely treatment and management

Created one of the largest Chinese BCD patient databases

We offered a promising practice of deep learning in retinal degenerative disease

Article

Quickly diagnosing Bietti crystalline dystrophy with deep learning

Haihan Zhang,[1,7] Kai Zhang,[2,7] Jinyuan Wang,[1,3] Shicheng Yu,[4] Zhixi Li,[5,6] Shiyi Yin,[1] Jingyuan Zhu,[1] and Wenbin Wei[1,8,*]

SUMMARY

Bietti crystalline dystrophy (BCD) is an autosomal recessive inherited retinal disease (IRD) and its early precise diagnosis is much challenging. This study aims to diagnose BCD and classify the clinical stage based on ultra-wide-field (UWF) color fundus photographs (CFPs) via deep learning (DL). All CFPs were labeled as BCD, retinitis pigmentosa (RP) or normal, and the BCD patients were further divided into three stages. DL models ResNeXt, Wide ResNet, and ResNeSt were developed, and model performance was evaluated using accuracy and confusion matrix. Then the diagnostic interpretability was verified by the heatmaps. The models achieved good classification results. Our study established the largest BCD database of Chinese population. We developed a quick diagnosing method for BCD and evaluated the potential efficacy of an automatic diagnosis and grading DL algorithm based on UWF fundus photography in a Chinese cohort of BCD patients.

INTRODUCTION

Bietti crystalline dystrophy (BCD, OMIM#210370), also known as Bietti crystalline retinopathy (BCR), is an autosomal recessive progressive retinal degenerative disease. This disease was first described in 1937 by Dr. Bietti.[1] The pathogenic gene is *CYP4V2* located at *4q35*, which encodes a protease related to lipid metabolism. *CYP4V2* is expressed in almost all human tissues, with particularly high levels in the retinal pigment epithelium (RPE) cells and retina photoreceptors.[2] BCD has a worldwide distribution and is especially common in East Asia; for example, China, Japan, and Korea. In Europe, most reported cases are from Italy and Spain.[3] International research suggests that the variant rate of BCD is approximately 1 in 67,000, and prevalence of 0.005 in China.[4] The disease is generally regarded as rare, and is often underdiagnosed. For example, a study by Mataftsi et al.[5] found that nearly 10% of patients diagnosed with retinitis pigmentosa (RP) may also be diagnosed with BCD.

BCD can be diagnosed by the following clinical features: visual field defects, numerous small flashy yellow-white intraretinal crystals, different degrees of RPE atrophy, retinal pigment masses, choroidal vascular sclerosis, visual field defects, rod and cone cell dysfunction showed on electroretinogram (ERG), and punctate hyperreflection on optical coherence tomography (OCT).[6] OCT can detect hyperreflective deposits in the complex of retina pigment epithelium-Bruch's membrane and disruption of the ellipsoid zone (EZ) in the eye. Intraretinal crystals did not exhibit any effect or any fluorescence and on fundus fluorescein angiography (FFA) or indocyanine green angiography (ICGA). In FFA, regions of RPE atrophy are linked to hyperfluorescent "window defects" where the choroidal capillaries remain mostly unaffected during the initial phase of the condition. Nevertheless, regions of decreased fluorescence in the lobules also align with inadequate blood flow in the choriocapillaris and degeneration of the chorioretinal layer as the disease progresses, with these regions of decreased fluorescence increasing in size gradually as time passes. The outcomes of ICGA differ based on the disease's progression. Initially, there were no alterations in RPE or loss of choriocapillaris; however, in later stages, there was notable chorioretinal atrophy seen as hypocyanescent areas.[7] Genetic testing can be used to confirm *CYP4V2* biallelic pathogenic variants if clinical features cannot clearly confirm the diagnosis.[6] Yuzawa et al.[8] divided BCD into 3 stages by observing the fundus manifestations. In 2020, Xu et al.[9] reported the results of gene variant detection in 138 Chinese BCD patients. They described the clinical features of the BCD patients along with various imaging examinations, and divide patients

[1]Beijing Tongren Eye Center, Beijing Key Laboratory of Intraocular Tumor Diagnosis and Treatment, Beijing Ophthalmology & Visual Sciences Key Lab, Medical Artificial Intelligence Research and Verification Key Laboratory of the Ministry of Industry and Information Technology, Beijing Tongren Hospital, Capital Medical University, Beijing, China
[2]Chongqing Chang'an Industrial Group Co. Ltd, Chongqing, China
[3]School of Clinical Medicine, Tsinghua University, Beijing, China
[4]Department of Ophthalmology, Beijing Key Laboratory of Restoration of Damaged Ocular Nerve, Peking University Third Hospital, Beijing, China
[5]State Key Laboratory of Ophthalmology, Zhongshan Ophthalmic Center, Sun Yat-sen University, Guangdong Provincial Key Laboratory of Ophthalmology and Visual Science, Guangzhou 510060, China
[6]Guangdong Provincial Clinical Research Center for Ocular Diseases, Guangzhou, China
[7]These authors contributed equally
[8]Lead contact
*Correspondence: weiwenbintr@163.com
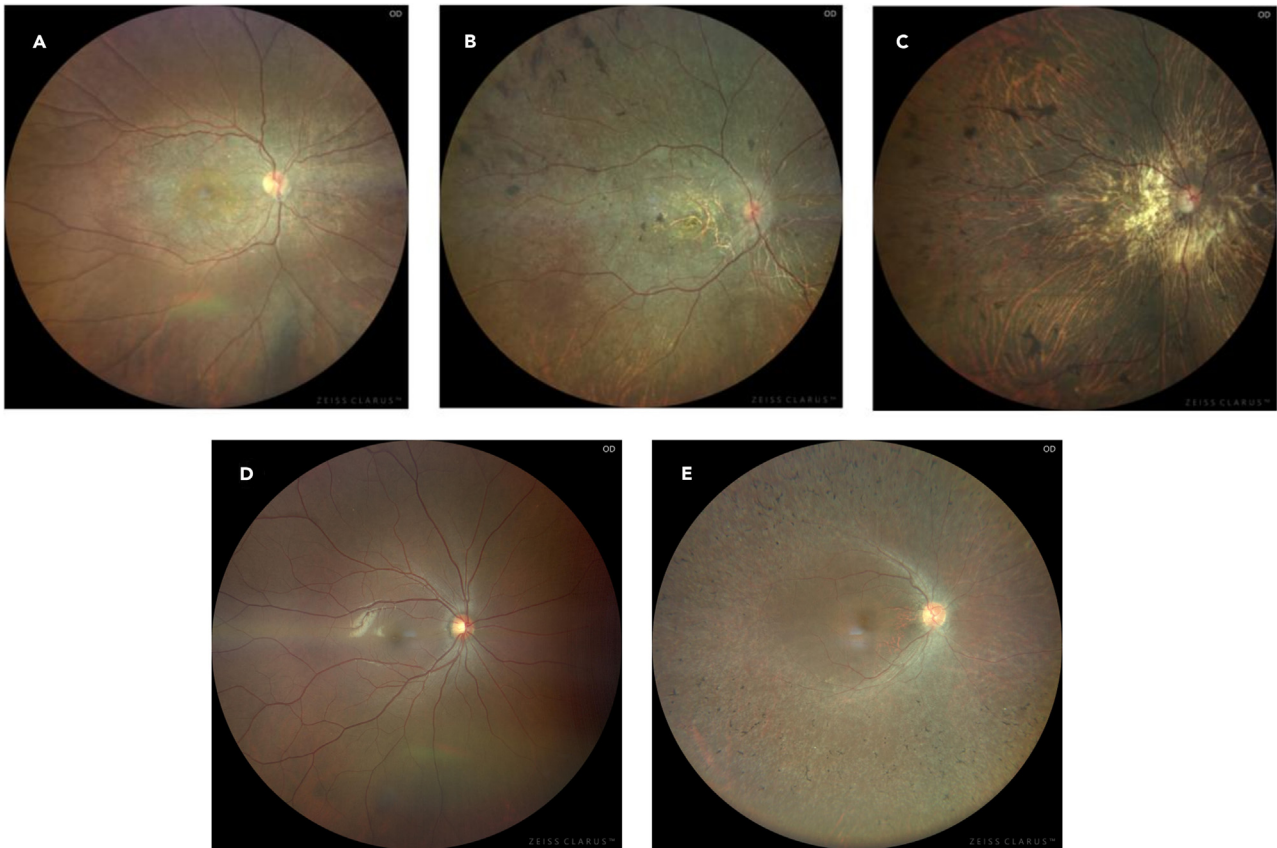https://doi.org/10.1016/j.isci.2024.110579

Figure 1. The most representative photos in the current study population were selected as a reference
(A–C) CFPs of typical stage 1, 2, and 3 BCD subjects; (D) normal fundus; (E) CFP of the RP subject.

into 3 stages based on the level of retinal crystal deposition and the severity of RPE and choroidal capillary degeneration as outlined by Yu-zawa et al.'s staging criteria.[8]

At present, there is no effective treatment for BCD patients in clinical practice. BCD was mainly treated according to typical RP and given supportive therapy such as vasodilators, vitamins, and traditional Chinese medicine. Given the recent success of gene therapy for inherited retinal diseases (IRDs), early detection of these diseases has become crucial.[10] This allows for prompt treatment and management. Due to their rarity in comparison to other eye conditions, ophthalmologists who have limited clinical experience may not recognize the symptoms of RP and BCD. Incorrect initial assessments or misinterpretations of fundus examination findings can lead to diagnostic errors. Therefore, better screening tools need to be developed.

Over the past few years, artificial intelligence (AI) techniques, especially deep learning (DL), have been utilized in analyzing OCT images and fundus photographs for the identification of retinal diseases such as diabetic retinopathy (DR), choroidal neovascularization (CNV), and age-related macular degeneration (AMD).[11–13] Numerous studies have also already utilized AI on OCT images for categorizing IRDs.[14–16] The Japan Eye Genetics Study (JEGC) Group, based on fundus photography and autofluorescence (FAF) imaging, has accurately forecasted genetic diagnoses for three types of conditions: Stargardt disease (ABCA4), occult macular dystrophy (RP1L1) and EYS gene-related retinitis pigmentosa.[17] Nevertheless, AI has not been utilized for the identification of BCD in fundus images. Because of its wide imaging range, fast imaging speed and high imaging resolution, ultra-wide-field (UWF) fundus photography plays a very important role in early diagnosis and intervention of ocular fundus diseases. In this study, we applied DL to develop a model that can automatically identify the clinical stage of BCD in UWF CFPs.

RESULTS

Characteristics of the patients

A total of 1,262 images from 166 BCD patients were retrospectively collected from Beijing Tongren Hospital during the period from May 2019 to January 2024. After manually excluding poor-quality images caused by halos, blurring, defocusing, etc., 1,138 images from 151 patients were finally included, with 139 (12.2%) images from 25 patients, 408 (35.9%) images from 53 patients, and 591 (51.9%) images from 73 patients were stage 1, 2, and 3 (as shown in Figure 1). As controls, we also included 502 fundus images from 76 RP patients and 180 fundus images from

Table 1. Basic demographic information of enrolled patients

Characteristic		Developmental dataset (Beijing Tongren Hospital)					External dataset (the Third Hospital of Peking University)		
		BCD							
		stage 1	stage 2	stage 3	RP	Normal	stage 1	stage 2	stage 3
Number of individuals		25	53	73	76	57	16	22	21
Total number of images		139	408	591	502	180	33	47	51
Sex	Male	10	22	47	40	32	9	15	18
	Female	15	31	26	36	25	7	7	3
Age (mean, y)		38.8	40.6	48.8	45.7	41.93	39.6	45.7	49.5

57 normal people without fundus disease. During the same period, 59 BCD patients in Peking University Third Hospital were enrolled, including 16 patients in stage 1, 22 patients in stage 2, and 21 patients in stage 3. Basic demographic information of included subjects is shown in Table 1. The age and gender distributions in the two datasets were not significantly different.

Performance of the deep learning algorithm

Tables 2 and 3 display the precise testing accuracy. To distinguish between the BCD, RP, and normal fundus, ResNeXt achieved a mean accuracy of 0.9850 ± 0.0250 (95% confidence intervals [CI] 0.9449–1.000) in the internal cross-validation dataset. Wide ResNet achieved a mean accuracy of 0.9812 ± 0.0197 (95% CI 0.9426–1.000), and ResNeSt achieved 0.9837 ± 0.0150 (95% CI 0.9543–1.000). To distinguish clinical stage of BCD patients, ResNeXt achieved a mean accuracy of 0.8899 ± 0.0873 (95% CI 0.618–0.9609), Wide ResNet achieved a mean accuracy of 0.7873 ± 0.0754 (95% CI 0.6394–0.9352), and ResNeSt achieved 0.7740 ± 0.0876 (95% CI 0.6024–0.9457) in the internal cross-validation dataset. In the external validation dataset, ResNeXt achieved an accuracy of BCD diagnosis was 1 (95% CI 0.9437–1.0000), and the accuracy of clinical staging was 0.5344 (95% CI 0.5011–0.5657). Wide ResNet achieved an accuracy of BCD diagnosis of 0.9924(95% CI 0.9364–1.0000), and the accuracy of clinical staging was 0.4962 (95% CI 0.4650–0.5276). ResNeSt achieved an accuracy of BCD diagnosis of 1 (95% CI 0.9437–1.0000), and the accuracy of clinical staging was 0.6260 (95% CI 0.5880–0.6568).

Table 2. Prediction accuracy of models

Model	Dataset	Accuracy (mean value ± standard deviation) [95% confidence interval]
ResNeXt	Internal cross validation (Differential Diagnosis of RP and BCD)	0.9850 ± 0.0250 [0.9449 1.0000]
	Internal cross validation (BCD classification)	0.8899 ± 0.0873 [0.6188 0.9609]
	External validation (Differential Diagnosis of RP and BCD)	1 [0.9437 1.0000]
	External validation (BCD classification)	0.5344 [0.5011 0.5657]
Wide ResNet	Internal cross validation (Differential Diagnosis of RP and BCD)	0.9812 ± 0.0197 [0.9426 1.0000]
	Internal cross validation (BCD classification)	0.7873 ± 0.0754 [0.6394 0.9352]
	External validation (Differential Diagnosis of RP and BCD)	0.9924 [0.9364 1.0000]
	External validation (BCD classification)	0.4962 [0.4650 0.5276]
ResNeSt	Internal cross validation (Differential Diagnosis of RP and BCD)	0.9837 ± 0.0150 [0.9543 1.0000]
	Internal cross validation (BCD classification)	0.7740 ± 0.0876 [0.6024 0.9457]
	External validation (Differential Diagnosis of RP and BCD)	1 [0.9437 1.0000]
	External validation (BCD classification)	0.6260 [0.5880 0.6568]

Ophthalmologists' performance was compared with 95% CI of the algorithm

Table 3. Prediction accuracy of models

Model	Dataset	Class	Accuracy	Sensitivity	Specificity
ResNeXt	Internal cross validation (Differential Diagnosis of RP and BCD)	Normal	1	1	1
		BCD	1	1	1
		RP	1	1	1
	Internal cross validation (BCD classification)	Stage 1	0.9076	0.7857	0.9238
		Stage 2	0.8571	0.7067	0.9264
		Stage 3	0.9580	0.9556	0.9612
	External validation (BCD classification)	Stage 1	1	0	0.7481
		Stage 2	0.5344	0.4468	0.5833
		Stage 3	0.7863	0.9608	0.6750
Wide ResNet	Internal cross validation (Differential Diagnosis of RP and BCD)	Normal	1	1	1
		BCD	1	1	1
		RP	1	1	1
	Internal cross validation (BCD classification)	Stage 1	0.9205	0.6207	0.9524
		Stage 2	0.8013	0.7119	0.8587
		Stage 3	0.8808	0.8516	0.9116
	External validation (BCD classification)	Stage 1	0.7634	0.0606	1
		Stage 2	0.6641	0.1985	0.9286
		Stage 3	0.5802	1	0.3125
ResNeSt	Internal cross validation (Differential Diagnosis of RP and BCD)	Normal	0.9969	1	0.9965
		BCD	0.9875	0.9800	1
		RP	1	1	1
	Internal cross validation (BCD classification)	Stage 1	0.8444	0	0.9341
		Stage 2	0.5166	0.6186	0.4511
		Stage 3	0.5033	0.3677	0.6463
	External validation (BCD classification)	Stage 1	0.6641	0.1515	0.8365
		Stage 2	0.5954	0.1277	0.8541
		Stage 3	0.4809	0.6863	0.3500

Confusion matrices of internal and external validation datasets (shown in Figures 2 and 3): each column represents prediction result of the algorithm; each row represents the expert labeling result; the values in matrix are normalized. Heatmap demonstrating representative fundus lesions (Figures 4 and 5): BCD fundus images mainly focused on yellow-white intraretinal crystal-like substances in the posterior pole, while RP fundus images focused on wax yellow optic disc and peripheral retinal osteocyte-like pigment deposition. In the late stage of BCD, the intra-retinal crystals were less and scattered, or almost absent. However, the retina and choroid were atrophic, and the choroidal vessels were exposed.

DISCUSSION

Recently, due to the characteristics of retinal immune avoidance, gene therapy has become a research hotspot of retinal genetic diseases and has shown good therapeutic prospects in preclinical animal models. To solve the treatment problem of IRD, early diagnosis and intervention treatment are crucial. Because the pathogenic gene of BCD is single and there is no genetic heterogeneity, the detection rate of gene variants in BCD patients is significantly higher than that in other hereditary retinopathy diseases.[18] *CYP4V2* is the only BCD gene identified so far. With the improvement of gene detection technology, new *CYP4V2* gene variant sites have been reported.[19] More than 100 variants have been identified in the *CYP4V2* gene to date.[20] In 2016, 17 variants of the *CYP4V2* gene linked to BCD were discovered through exon sequencing and Sanger sequencing in 36 Chinese families, involving 68 pairs of alleles. The most prevalent variants in China were c.802-8_810del17b-pinsGC, c.802-8_810del17bpinsGT, c.992A>C (p.H331P), and c.1091-2A>G, making up 71% of the mutant alleles.[2]

Marginal crystalline keratopathy in patients with BCD, which is composed of smaller than 15 μm of refringent subepithelial limbal deposits, can easily be missed or masked by the presence of arcus senilis even by experienced ophthalmologists. Clinically, stage 1 and stage 2 patients have obvious yellow-white crystalline substances in the fundus, which is easy to make a clear diagnosis. However, for some stage 3 patients, with the decrease of typical crystalline substances in the fundus, it is relatively difficult to make a clear diagnosis, and sometimes it is difficult to
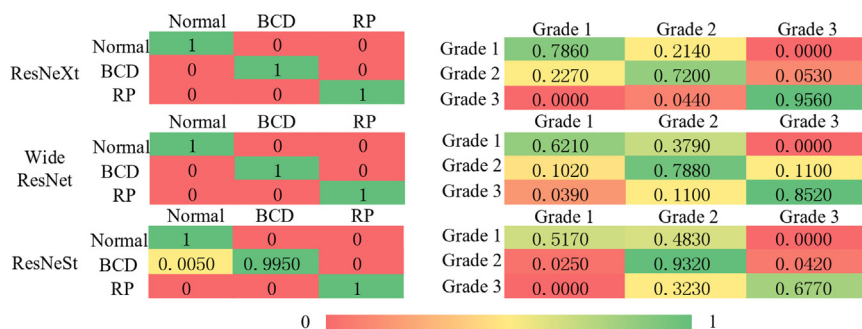
Figure 2. Confusion matrix: differential diagnosis of RP and BCD and the grading of BCD in internal cross validation dataset

distinguish from other diffuse choroidal sclerosis conditions. For such patients, the detection and determination of the corresponding *CYP4V2* gene variant is particularly important.

Next-generation sequencing (NGS), also referred to as high-throughput sequencing, is a method of DNA sequencing that utilizes PCR and gene chips. NGS is characterized by high throughput and a slightly higher error rate, which has greatly improved the efficiency of disease research and provided a more effective means for the research, diagnosis, and treatment of diseases. However, NGS still has some problems to be solved, including technical limitations, clinical application, high cost, and the current lack of interpretation guidelines for clinicians. The high cost of testing and long waiting time often discourage patients, and even miss the best opportunity for intervention. With further developments, AI model may be a diagnostic tool and may give relevant information for future therapeutic approaches.

AI has been leading the way in ophthalmology when it comes to retinal disorders. A growing number of research groups around the world are focusing on AI, using multiple imaging modalities and a range of AI models to assist in all aspects of patient care, including diagnosis, triage, grading, and prognosis.[21,22] AI has broad prospects in coping with medical staff shortages and improving preventable diseases. To date, there have been few studies using DL to classify fundus images of RP patients in the literature (Table 4). To detect RP from CFPs, Chen et al.[23] developed and evaluated a transfer-learning model. A total of 1,670 CFPs were obtained and analyzed from the Taiwan project on inherited retinal degeneration and the National Taiwan University Hospital. The model achieved a peak accuracy of 96.00% and an area under the receiver operating characteristic (AUROC) of 96.74%. Traditional machine learning algorithms need to extract features from images before learning, while the convolutional layer in DL automatically mines features of image data during the learning process. In contrast to conventional machine learning, which relies on manually designed features based on human domain-specific knowledge, DL techniques have the ability to leverage all the data present within the image itself, giving them a fundamental edge over traditional methods. Since the typical features in the fundus images of BCD patients are too small to be labeled, we use this advantage of DL to greatly simplify the difficulty of calculation.

To the best of our knowledge, this study has created the most extensive BCD databases for Chinese individuals, and we plan to store the code and data in a publicly accessible repository. Our study validated the application value of DL in the diagnosis and clinical staging of BCD from CFPs. Based on UWF fundus photography, DL methods were tested on a Chinese cohort of BCD patients. We compared the performance of several architectures, including ResNeXt, Wide ResNet, and ResNeSt. In the diagnosis of BCD, the automatic classification was highly accurate of all three models. To distinguish clinical stage of BCD patients, ResNeXt achieved a best accuracy of 0.8899 ± 0.0873 (95% CI 0.618–0.9609) in the internal cross-validation dataset. ResNeSt achieved a best accuracy of 0.6260 (95% CI 0.5880–0.6568) in the external validation dataset. Our study illustrates the potential efficacy of an automated diagnosis/grading system for BCD based on fundus photography. Firstly, early detection can help patients receive further counseling and treatment for BCD, a retinal disease that can result in irreversible blindness. Compared with other eye diseases, BCD is relatively rare and is a hard diagnosed disease for many young and primary
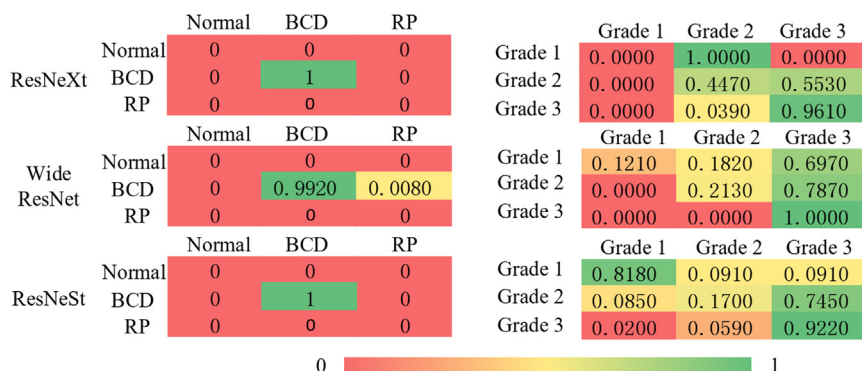

Figure 3. Confusion matrix: differential diagnosis of RP and BCD and the grading of BCD in external validation dataset

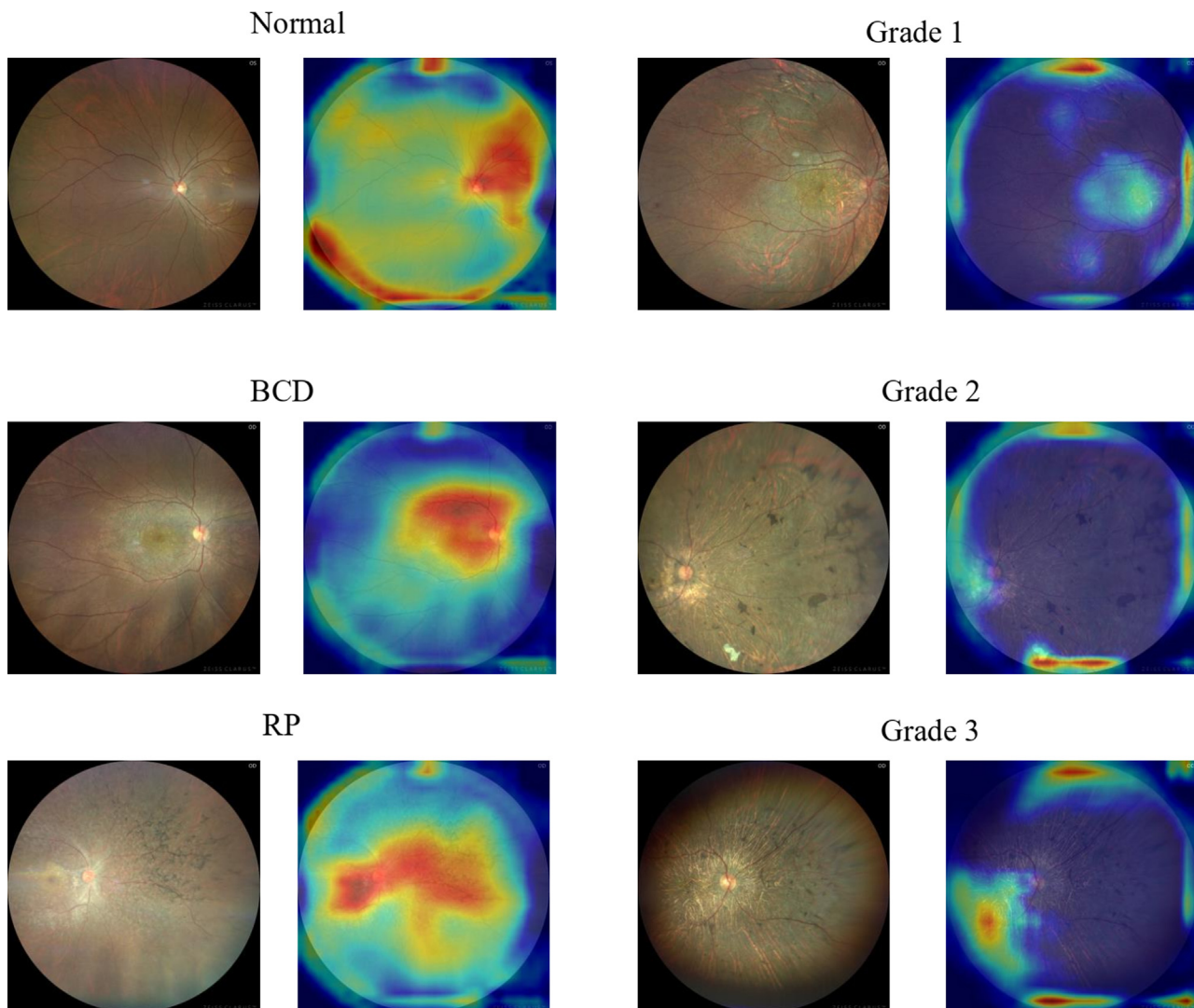Normal

Grade 1

BCD

Grade 2

RP

Grade 3

Figure 4. Heatmap visualization of internal dataset

ophthalmologists. Based on the study, we may provide convenience for clinical work and further improve the clinical detection rate of BCD. In addition, BCD is a genetic disorder, and early awareness of this can also help family planning and reduce the prevalence of BCD.

At the same time, there are still many challenges for AI implements in ophthalmology. In clinical settings, obtaining sufficient high-quality training data for automated image analysis with DL can be difficult. With little understanding of these genetic conditions, obtaining large amounts of data in patients with BCD is even more difficult. Therefore, we used a relatively small dataset. In the future, efforts are needed among domestic and international ophthalmologists to establish a comprehensive image grading consensus for specific diseases. Multi-center, international collaborations hold promise for expanding the algorithm performance. Further investigation is required for the application of AI in eye diseases, including the utilization of multiple types of data to select suitable participants for clinical trials, as well as evaluating functional limitations using structural measurements in IRD.

Overall, we have found wide-field CFPs to be an effective non-invasive method for diagnosing and grading BCDs. We generate a DL-based algorithm trained using CFPs that is highly sensitive and specific for identifying BCD patients. In our knowledge, this study is the initial attempt to assess the capability of DL in automating the detection of BCD using CFPs. The practical feasibility for clinical application of this algorithm needs to be further studied.

Limitations of the study

There are some limitations in this study. First, compared to other machine learning models, the study sample did not include people from multiple ethnicities and regions. Then, the control group we included did not have any fundus disease. Follow-up studies may consider
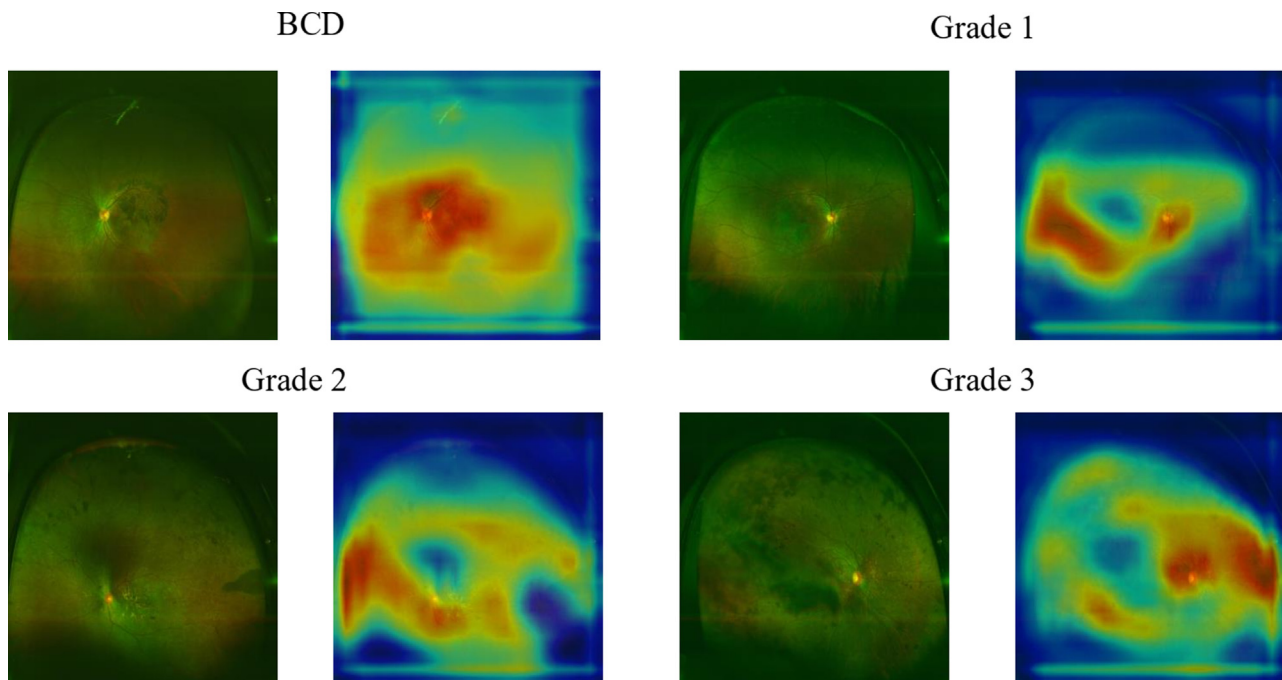
Figure 5. Heatmap visualization of external validation dataset

including some patients with other types of fundus disease that are easily confused with RP/BCD as a control group, for example, Macular Dystrophy, Stargardt disease, the Best's Disease, and more. Due to the limitation of image quality,[26] only the BCD fundus image data are available in the external verification dataset, and a more complete external dataset used to test the algorithm may produce more optimistic results. We once considered the incorporation of autofluorescent images and OCT parameters into AI diagnosis, but this could not be achieved due to some objective conditions and technical reasons. In addition, the wide-field fundus photographs from two medical centers included in this study were from different fundus photographic instruments (CLARUS 500, ZEISS, Germany and Panoramic Ophthalmoscope, Optos, Britain). The two commercial UWF fundus cameras are generated from different theories, thus showed different characteristics, in color, ratio, etc., which brought classification errors to some extent. The confusion matrix plot shows that the overall classification performance of the models for the clinical stages of BCD patients is not very good. However, the vast majority of images with incorrect classification results were classified as advanced grades, which is a low-risk condition for BCD patients, meaning that our models are unlikely to miss severe lesions. The staging of the disease is difficult and subjective, so we think this result is acceptable. It still needs more insights on the results of this study to see whether it is applicable to other fundus cameras. We will continue to collect multimodal image data of BCD patients to explore whether it is effective to improve the accuracy of AI algorithms.

STAR★METHODS

Detailed methods are provided in the online version of this paper and include the following:

- KEY RESOURCES TABLE
- RESOURCE AVAILABILITY
  - Lead contact
  - Materials availability
  - Data and code availability
- EXPERIMENTAL MODEL AND STUDY PARTICIPANT DETAILS
- METHOD DETAILS
  - Images quality control and labeling
  - Development of deep learning algorithm
  - Validation of deep learning algorithm
- QUANTIFICATION AND STATISTICAL ANALYSIS
- ADDITIONAL RESOURCES

Table 4. Previous relevant study analysis

Reference	Disease type (s)	Imaging modality	Dataset size	Sample size	AI Problem	Algorithm	Model (s)	Best performance
Camino et al.[14]	Retinitis pigmentosa (RP), chloridemia	Optical coherence Tomography (OCT)	20 OCT scans	22 RP and 20 chloridemia subjects	Segmentation	CNNs (convolutional neural networks)	MatConvNet	JSI (Jaccard similarity index):0.912 $\pm$ 0.055
Fujinami-Yokokawa et al.[15]	RP, macular dystrophy	Spectral domain Optical coherence Tomography (SD-OCT)	178 SD-OCT scans	28 RP, 30 macular dystrophy, and 17 healthy subjects	Classification	DNNs (deep neural networks)	InceptionV3	Accuracy: 1.0
Iadanza et al.[24]	RP	Pupillometer	30 chromatic pupillometry data	28 RP, and 10 healthy subjects	Classification	Feature extraction, SVM (support vector machine)	Linear SVM, Gaussian radialbasis function (RBF)	Accuracy: 0.846, Sensitivity: 0.937, Specificity: 0.786
Miere et al.[25]	RP, Best's disease (BD), Stargardt disease (STGD)	Fundus autofluorescence (FAF)	483 images	160 RP,125 BD eyes,125 STGD, and 73 healthy subjects	Classification	CNNs	ResNet101	ROC - AUC (Receiver Operating Characteristic Curve - Area under the Curve): 0.999, PRC-AUC: 0.999
Chen et al.[23]	RP	Fundus photography	1,670 images	1153 RP, and 517 healthy eyes	Classification	CNNs	InceptionV3, Inception-ResNetV2, and Xception	Accuracy: 0.960, AUROC: 0.9946, Sensitivity: 0.9571 Specificity: 0.9853 F3: 0.9599

REFERENCES

1. Bietti, G. (1937). Ueber familiares Vorkommen von" Retinitis punkutata albescens"(verbunden mit" Dystrophia marginalis cristallinea corneae"), Glitzern des Glaskorpers und anderen degenerativen Augenveranderungen. Klin. Monatsbl. Augenheilkd. *99*, 737–756.

2. Li, A., Jiao, X., Munier, F.L., Schorderet, D.F., Yao, W., Iwata, F., Hayakawa, M., Kanai, A., Shy Chen, M., Alan Lewis, R., et al. (2004). Bietti crystalline corneoretinal dystrophy is caused by mutations in the novel gene CYP4V2. Am. J. Hum. Genet. *74*, 817–826. https://doi.org/10.1086/383228.

3. García-García, G.P., Martínez-Rubio, M., Moya-Moya, M.-A., Pérez Santonja, J.J., and Escribano, J. (2019). Current perspectives in Bietti crystalline dystrophy. Clin. Ophthalmol. *13*, 1379–1399. https://doi.org/10.2147/opth.S185744.

4. Shan, M., Dong, B., Zhao, X., Wang, J., Li, G., Yang, Y., and Li, Y. (2005). Novel mutations in the CYP4V2 gene associated with Bietti crystalline corneoretinal dystrophy. Mol. Vis. *11*, 738–743.

5. Mataftsi, A., Zografos, L., Millá, E., Secrétan, M., and Munier, F.L. (2004). Bietti's crystalline corneoretinal dystrophy: a cross-sectional study. Retina *24*, 416–426. https://doi.org/10.1097/00006982-200406000-00013.

6. Vargas, M., Mitchell, A., Yang, P., and Weleber, R. (2019). Bietti Crystalline Dystrophy.

7. Saatci, A.O., Yaman, A., Öner, F.H., Ergin, M.H., and Çingil, G. (2002). Indocyanine green angiography in Biettils crystalline retinopathy. Can. J. Ophthalmol. *37*, 346–351.

8. Yuzawa, M., Mae, Y., and Matsui, M. (1986). Bietti's crystalline retinopathy. Ophthalmic Paediatr. Genet. *7*, 9–20. https://doi.org/10.3109/13816818609058037.

9. Ke, X., Xiaohui, Z., Yue, X., Hanwen, Y., Bing, Y., and Yang, L. (2020). Clinical features of Bietti crystalline corneoretinal dystrophy caused by mutations in the CYP4V2 gene. Ophthalmol. China *29*, 93.

10. Wang, J., Zhang, J., Yu, S., Li, H., Chen, S., Luo, J., Wang, H., Guan, Y., Zhang, H., Yin, S., et al. (2024). Gene replacement therapy in Bietti crystalline corneoretinal dystrophy: an open-label, single-arm, exploratory trial. Signal Transduct. Target. Ther. *9*, 95. https://doi.org/10.1038/s41392-024-01806-3.

11. Gulshan, V., Peng, L., Coram, M., Stumpe, M.C., Wu, D., Narayanaswamy, A., Venugopalan, S., Widner, K., Madams, T., Cuadros, J., et al. (2016). Development and Validation of a Deep Learning Algorithm for Detection of Diabetic Retinopathy in Retinal Fundus Photographs. JAMA *316*, 2402–2410. https://doi.org/10.1001/jama.2016.17216.

12. Lee, C.S., Tyring, A.J., Deruyter, N.P., Wu, Y., Rokem, A., and Lee, A.Y. (2017). Deep-learning based, automated segmentation of macular edema in optical coherence tomography. Biomed. Opt Express *8*, 3440–3448. https://doi.org/10.1364/boe.8.003440.

13. Burlina, P.M., Joshi, N., Pekala, M., Pacheco, K.D., Freund, D.E., and Bressler, N.M. (2017). Automated Grading of Age-Related Macular Degeneration From Color Fundus Images Using Deep Convolutional Neural Networks. JAMA Ophthalmol. *135*, 1170–1176. https://doi.org/10.1001/jamaophthalmol.2017.3782.

14. Camino, A., Wang, Z., Wang, J., Pennesi, M.E., Yang, P., Huang, D., Li, D., and Jia, Y. (2018). Deep learning for the segmentation of preserved photoreceptors on *en face* optical coherence tomography in two inherited retinal diseases. Biomed. Opt Express *9*, 3092–3105. https://doi.org/10.1364/boe.9.003092.

15. Fujinami-Yokokawa, Y., Pontikos, N., Yang, L., Tsunoda, K., Yoshitake, K., Iwata, T., Miyata, H., Fujinami, K., and Japan Eye Genetics Consortium, O.B.O. (2019). Japan Eye Genetics Consortium OBO (2019). Prediction of Causative Genes in Inherited Retinal Disorders from Spectral-Domain Optical Coherence Tomography Utilizing Deep Learning Techniques. J. Ophthalmol. *2019*, 1691064. https://doi.org/10.1155/2019/1691064.

16. Kermany, D.S., Goldbaum, M., Cai, W., Valentim, C.C.S., Liang, H., Baxter, S.L., McKeown, A., Yang, G., Wu, X., Yan, F., et al. (2018). Identifying Medical Diagnoses and Treatable Diseases by Image-Based Deep Learning. Cell *172*, 1122–1131.e9. https://doi.org/10.1016/j.cell.2018.02.010.

17. Fujinami-Yokokawa, Y., Ninomiya, H., Liu, X., Yang, L., Pontikos, N., Yoshitake, K., Iwata, T., Sato, Y., Hashimoto, T., Tsunoda, K., et al. (2021). Prediction of causative genes in inherited retinal disorder from fundus photography and autofluorescence imaging using deep learning techniques. Br. J. Ophthalmol. *105*, 1272–1279. https://doi.org/10.1136/bjophthalmol-2020-318544.

18. Meng, X.H., He, Y., Zhao, T.T., Li, S.Y., Liu, Y., and Yin, Z.Q. (2019). Novel mutations in CYP_4V2 in Bietti corneoretinal crystalline dystrophy: Next-generation sequencing technology and genotype-phenotype correlations. Mol. Vis. *25*, 654–662.

19. Lin, J., Nishiguchi, K.M., Nakamura, M., Dryja, T.P., Berson, E.L., and Miyake, Y. (2005). Recessive mutations in the CYP4V2 gene in East Asian and Middle Eastern patients with Bietti crystalline corneoretinal dystrophy. J. Med. Genet. *42*, e38. https://doi.org/10.1136/jmg.2004.029066.

20. Saatci, A.O., Ataş, F., Çetin, G.O., and Kayabaşı, M. (2023). Diagnostic and Management Strategies of Bietti Crystalline Dystrophy: Current Perspectives. Clin. Ophthalmol. *17*, 953–967.

21. Keenan, T.D.L., Chen, Q., Peng, Y., Domalpally, A., Agrón, E., Hwang, C.K., Thavikulwat, A.T., Lee, D.H., Li, D., Wong, W.T., et al. (2020). Deep Learning Automated Detection of Reticular Pseudodrusen from Fundus Autofluorescence Images or Color Fundus Photographs in AREDS2. Ophthalmology *127*, 1674–1687. https://doi.org/10.1016/j.ophtha.2020.05.036.

22. De Fauw, J., Ledsam, J.R., Romera-Paredes, B., Nikolov, S., Tomasev, N., Blackwell, S., Askham, H., Glorot, X., O'Donoghue, B., Visentin, D., et al. (2018). Clinically applicable deep learning for diagnosis and referral in

retinal disease. Nat. Med. *24*, 1342–1350. https://doi.org/10.1038/s41591-018-0107-6.

23. Chen, T.-C., Lim, W.S., Wang, V.Y., Ko, M.-L., Chiu, S.-I., Huang, Y.-S., Lai, F., Yang, C.-M., Hu, F.-R., Jang, J.-S.R., and Yang, C.H. (2021). Artificial intelligence–assisted early detection of retinitis pigmentosa—the most common inherited retinal degeneration. J. Digit. Imaging *34*, 948–958.

24. Iadanza, E., Goretti, F., Sorelli, M., Melillo, P., Pecchia, L., Simonelli, F., and Gherardelli, M. (2020). Automatic detection of genetic diseases in pediatric age using pupillometry. IEEE Access *8*, 34949–34961.

25. Miere, A., Le Meur, T., Bitton, K., Pallone, C., Semoun, O., Capuano, V., Colantuono, D., Taibouni, K., Chenoune, Y., Astroz, P., et al. (2020). Deep Learning-Based Classification of Inherited Retinal Diseases Using Fundus Autofluorescence. J. Clin. Med. *9*, 3303. https://doi.org/10.3390/jcm9103303.

26. Zhang, Y., Zhang, K., Ding, Y., Liu, S., Wang, M., Wang, X., Qin, Z., Zhang, X., Ma, T., Hu, F., et al. (2023). Deep transfer learning from ordinary to capsule esophagogastroduodenoscopy for image quality controlling. Eng. Rep. 6, e12776.

27. Zhang, K., Zhang, Y., Ding, Y., Wang, M., Bai, P., Wang, X., Qin, Z., Zhang, X., Ma, T., Hu, F., et al. (2024). Anatomical sites identification in both ordinary and capsule gastroduodenoscopy via deep learning. Biomed. Signal Process Control *90*, 105911. https://doi.org/10.1016/j.bspc.2023.105911.

28. Du, K., Dong, L., Zhang, K., Guan, M., Chen, C., Xie, L., Kong, W., Li, H., Zhang, R., and Zhou, W. (2024). Deep Learning System for Screening AIDS-related Cytomegalovirus Retinitis with Ultra-Wide-Field Fundus Images. Heliyon *10*, e30881.

29. Hui, S., Dong, L., Zhang, K., Nie, Z., Jiang, X., Li, H., Hou, Z., Ding, J., Wang, Y., and Li, D. (2022). Noninvasive identification of Benign and malignant eyelid tumors using clinical images via deep learning system. J. Big Data *9*, 84.

30. Zhou, W.-D., Dong, L., Zhang, K., Wang, Q., Shao, L., Yang, Q., Liu, Y.-M., Fang, L.-J., Shi, X.-H., Zhang, C., et al. (2022). Deep Learning for Automatic Detection of Recurrent Retinal Detachment after Surgery Using Ultra-Widefield Fundus Images: A Single-Center Study. Adv. Intell. Syst. *4*, 2200067.

31. Pan, Q., Zhang, K., He, L., Dong, Z., Zhang, L., Wu, X., Wu, Y., and Gao, Y. (2021). Automatically Diagnosing Disk Bulge and Disk Herniation With Lumbar Magnetic Resonance Images by Using Deep Convolutional Neural Networks: Method Development Study. JMIR Med. Inform. *9*, e14755. https://doi.org/10.2196/14755.

32. Zhang, K., Liu, X., Liu, F., He, L., Zhang, L., Yang, Y., Li, W., Wang, S., Liu, L., Liu, Z., et al. (2018). An Interpretable and Expandable Deep Learning Diagnostic System for Multiple Ocular Diseases: Qualitative Study. J. Med. Internet Res. *20*, e11144. https://doi.org/10.2196/11144.

33. Li, Z., Guo, C., Nie, D., Lin, D., Zhu, Y., Chen, C., Zhao, L., Wu, X., Dongye, M., Xu, F., et al. (2020). Deep learning from "passive feeding" to "selective eating" of real-world data. NPJ Digit. Med. *3*, 143. https://doi.org/10.1038/s41746-020-00350-y.

34. Shorten, C., Khoshgoftaar, T.M., and Furht, B. (2021). Text Data Augmentation for Deep Learning. J. Big Data *8*, 101. https://doi.org/10.1186/s40537-021-00492-0.

35. Xie, S., Girshick, R., Dollár, P., Tu, Z., and He, K. (2017). Aggregated Residual Transformations for Deep Neural Networks. In Proceedings of the IEEE conference on computer vision and pattern recognition: 2017, pp. 1492–1500.

36. Zhang, H., Wu, C., Zhang, Z., Zhu, Y., Lin, H., Zhang, Z., Sun, Y., He, T., Mueller, J., and Manmatha, R. (2022). Resnest: Split-Attention Networks. In Proceedings of the IEEE/CVF conference on computer vision and pattern recognition: 2022, pp. 2736–2746.

37. Zagoruyko, S., and Komodakis, N. (2016). Wide Residual Networks. Preprint at arXiv. https://doi.org/10.48550/arXiv.1605.07146.

38. Lu, B., Li, H.-X., Chang, Z.-K., Li, L., Chen, N.-X., Zhu, Z.-C., Zhou, H.-X., Li, X.-Y., Wang, Y.-W., Cui, S.-X., et al. (2022). A practical Alzheimer's disease classifier via brain imaging-based deep learning on 85,721 samples. J. Big Data *9*, 101.

39. Zhang, M., Zhang, K., Yu, D., Xie, Q., Liu, B., Chen, D., Xv, D., Li, Z., and Liu, C. (2021). Computerized assisted evaluation system for canine cardiomegaly via key points detection with deep learning. Prev. Vet. Med. *193*, 105399. https://doi.org/10.1016/j.prevetmed.2021.105399.

40. Deng, J., Dong, W., Socher, R., Li, L.-J., Li, K., and Fei-Fei, L. (2009). Imagenet: A Large-Scale Hierarchical Image Database. In 2009 IEEE conference on computer vision and pattern recognition: 2009 (IEEE), pp. 248–255.

41. Bottou, L. (2012). Stochastic Gradient Descent Tricks. In Neural Networks: Tricks of the Trade: Second Edition (Springer), pp. 421–436.

42. Zhang, R., Dong, L., Li, R., Zhang, K., Li, Y., Zhao, H., Shi, J., Ge, X., Xu, X., Jiang, L., et al. (2023). Automatic retinoblastoma screening and surveillance using deep learning. Br. J. Cancer *129*, 466–474. https://doi.org/10.1038/s41416-023-02320-z.

43. Selvaraju, R.R., Cogswell, M., Das, A., Vedantam, R., Parikh, D., and Batra, D. (2017). Grad-CAM: Visual Explanations from Deep Networks via Gradient-Based Localization. In 2017 IEEE International Conference on Computer Vision (ICCV), pp. 618–626.

44. Schmidt, H., Spieker, A.J., Luo, T., Szymczak, J.E., and Grande, D. (2021). Variability in Primary Care Physician Attitudes Toward Medicaid Work Requirement Exemption Requests Made by Patients With Depression. JAMA Health Forum *2*, e212932. https://doi.org/10.1001/jamahealthforum.2021.2932.

45. Lott, A., and Reiter, J.P. (2020). Wilson confidence intervals for binomial proportions with multiple imputation for missing data. Am. Statis. *74*, 109–115.

STAR★METHODS

KEY RESOURCES TABLE

REAGENT or RESOURCE	SOURCE	IDENTIFIER
Deposited data		
Raw fundus photographs data	This paper	N/A
Code for model and network training and analysis	This paper	https://github.com/Hugo0512/AI4BCD https://github.com/MachineLP/PyTorch_image_classifier
Software and algorithms		
ResNeXt32 × 8d	TorchVision Package	https://github.com/Hugo0512/AI4BCD
Wide ResNet	TorchVision Package	https://github.com/Hugo0512/AI4BCD
ResNeSt	TorchVision Package	https://github.com/MachineLP/PyTorch_image_classifier
PyTorch (version 1.8.1)	PyTorch Software Foundation	https://pytorch.org/
MATLAB R2016a	MATLAB Software Foundation	https://ww2.mathworks.cn/

RESOURCE AVAILABILITY

Lead contact

Further information and requests for resources should be directed to and will be fulfilled by the lead contact, Wenbin Wei (weiwenbintr@163.com).

Materials availability

This paper did not generate new unique materials.

Data and code availability

- Fundus photographs data reported in this paper will be shared by the lead contact upon request.
- All original code is available in https://github.com/Hugo0512/AI4BCD and https://github.com/MachineLP/PyTorch_image_classifier. All relevant data and materials have been included in the manuscript.
- Any additional information required to reanalyze the data reported in this paper is available from the lead contact upon request.

EXPERIMENTAL MODEL AND STUDY PARTICIPANT DETAILS

The fundus images used in this study originated from patients diagnosed with BCD or RP at Beijing Tongren Hospital between 2019 and 2024, and external verification images obtained from the Third Hospital of Peking University. All BCD patients were confirmed with *CYP4V2* gene variants by genetic testing. As the control group, the normal subjects with diopter between −3.0D and +3.0D were checked without any fundus or optic nerve diseases. The study was approved by the Ethics Review Committees of Beijing Tongren Hospital and Peking University Third Hospital, and participants provided written informed consent.

METHOD DETAILS

Images quality control and labeling

Our study is of the retrospective nature. All UWF fundus photographs were captured with commercial available equipment (CLARUS 500, ZEISS, Germany; Panoramic Ophthalmoscope, Optos, Britain) and stored in.jpg or.tiff formats in the imaging database. Low-quality photographs[27] resulting from halation, blur, defocus or severe opacity of the refractive stroma were all excluded manually.[28] A total of 1138 fundus photographs of BCD patients, 502 of RP patients, and 180 of normal fundus images were included as developmental set. Multiple fundus photographs focusing on the nasal and temporal retinas were obtained for each patient in each eye. In addition, there are 131 images of BCD patients from Peking University Third Hospital were included as external validation dataset. Identical exclusion criteria were applied to patients in both centers: previous fundus surgery or laser treatment; combined with other ophthalmic diseases, such as macular degeneration, diabetic or hypertensive retinopathy, glaucoma, uveitis, retinal detachment, epiretinal membrane, macular hole, macular neovascularization, optic neuropathy, and etc. These conditions often affect the graphic interpretation of fundus images by clinicians or AI algorithms.

All included fundus photographs were classified into three categories: "normal", "BCD" and "RP" according to the patients' clinical diagnosis and genetic test results. Furthermore, the demographic information of the BCD patients was masked and the images were graded by three ophthalmologists, including two junior ophthalmologists and one senior ophthalmologist. Referring to the staging criteria of Xu et al.,[9]

all included BCD patients were divided into 3 stages. In stage 1, the RPE was slightly atrophied, and fine granular yellow-white crystals were deposited in the macular area. In stage 2, there was a high concentration of crystals deposited throughout the entire fundus, extending beyond the macular region, with noticeable atrophy of the RPE and choroidal capillaries in that area. Gradually, stage 3 saw the crystalline deposits subsided, the number and distribution of crystalline deposits varied among individuals, and obvious atrophy of RPE and choroid could be observed throughout the fundus. Patients in stages 1–3 may have visual field defects, which are manifested as central, paracentral, or irregular scotoma. Two junior ophthalmologists labeled each image (HH Zhang and JY Wang). Disagreements were arbitrated by a senior ophthalmologist (WB Wei).

Development of deep learning algorithm

Fundus photographs from Beijing Tongren Hospital were partitioned randomly into training datasets and internal validation sets using 5-fold cross-validation to create and assess the effectiveness of the DL model.[29,30] Cross-validation is performed in a subject independent way, ensuring that the images from a single patient are not split into training and validation sets. We initially compared the effectiveness of various architectures, such as ResNet-101, ResNeXt32 × 8d, InceptionV3, Wide ResNet and ResNeSt,[31–37] for automatically differentiating normal fundus, RP, and BCD, as well as automatically classifying BCD patients. ResNeXt32 × 8d, Wide ResNet and ResNeSt perform better and was selected to complete the task. UWF images were used as input for the model. The first three classes classification model distinguishes between normal fundus, RP and BCD. The second three classes classification model distinguishes BCD eyes with different severity. We did not apply data augmentation to all models, and the model with the best performance in the internal cross-validation was used for testing with the external validation dataset.[38,39] All models were developed using PyTorch 1.8.1 on a server with two NVIDIA 3090 Graphical Processing Units.[40] Before inputting into the model for training or testing, all images are adjusted to a size of 1024 × 1024 and all pixel values are standardized to fall within the range of [0,1]. The optimized algorithm was SGD (Stochastic Gradient Descent),[41] utilizing the standard hyperparameters in PyTorch 1.8.0, with a batch size of 6. In addition, the class weight was used to weigh the influence of the unbalanced distribution of different categories.[42] As a result of repeated experiments, 10 epochs were used to train the model without underfitting. The model with the best validation accuracy was saved as the final model for deployment.

Validation of deep learning algorithm

In the first step, using an internal cross-validation dataset, we validated the algorithm's performance in identifying patients with BCD. Then for further performance evaluation, 131 fundus photographs of 59 BCD patients from another medical center, the Third Hospital of Peking University, were independently classified regardless of patient demographics and final multidisciplinary management strategy, and their results were compared with those of our algorithm. Two models are used. The first is used to distinguish BCD, RP and normal fundus image, and the second is used to grade BCD.

QUANTIFICATION AND STATISTICAL ANALYSIS

In order to understand the decision-making process of the model, we utilized Grad-CAM to produce heatmaps.[43] Since both of our algorithms are three classes classification problems (multi-classification), row normalized confusion matrix and accuracy are used to evaluate the performance. The model's overall performance and the identification of each category were evaluated using accuracy and confusion matrix, respectively. In internal cross-validation datasets, the corresponding CI were calculated using point estimates.[44] In external validation dataset, Wilson confidence interval was used to estimate the confidence interval.[45] All statistical analysis was performed using MATLAB R2016a. Toward each specific class, we evaluate the accuracy, specificity and sensitivity.

ADDITIONAL RESOURCES

This study did not use any type of experimental models. The study was conducted with the approval of the Medical Ethics Committee of Beijing Tongren Hospital (reference number: TREC2022-120) and the Third Hospital of Peking University (reference number: 2022-265-02). During the retrospective collection process, personal information that could identify individuals was eliminated. The informed consent was signed by all patients.